Photons as tracers of the curvature of space-time and the mass distribution in the Universe

Laurent Magri-Stella[1,2], Narei Lorenzo Martinez[2,3], Vincent Reverdy[2,3]

[1] Université Savoie Mont Blanc
[2] Laboratoire d'Annecy de Physique des Particules (LAPP), CNRS
9 Chemin de Bellevue, 74940 Annecy-le-Vieux
[3] Centre National de la Recherche Scientifique (CNRS)

04.11.2025

A questioned cosmology: ΛCDM

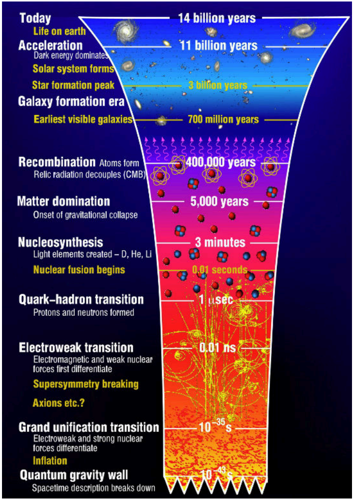

Figure 1: Illustration of the ΛCDM model.

Param.	Desc.
$\Omega_b h^2$	Baryon density
$\Omega_c h^2$	Dark matter density
H_0	Hubble constant
τ	Optical depth (reionization)
n_s	Scalar spectral index
A_s	Power spectrum amplitude

Table 1: The six base parameters of the ΛCDM model

A questioned cosmology: ΛCDM

Probe	**Parameters**	**Measurements**
CMB	H_0, Ω_m, n_s	Temperature anisotropies
SN Ia	H_0	Luminosity distances
BAO	H_0, Ω_m	Galaxy correlation scale
Galaxy clusters	Ω_m, σ_8	Mass, spatial distribution

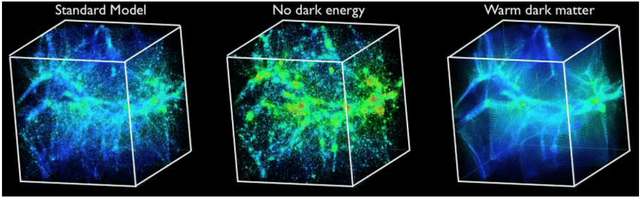

(a) Matter distribution changes with different cosmological models
Credit: K. Heitmann

(b) Abell 370
NASA/ESA

Inferring cosmology from the Universe's mass distribution

One quantity, many ways to measure it

- Mass-richness relations
- X-ray luminosity
- Number counts
- Sunyaev-Zel'dovich signal
- Weak lensing
- In simulations: Friends-of-Friends, M_{200}

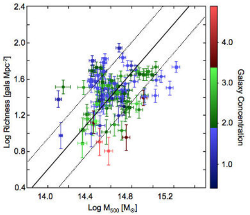

(a) Example of a mass-richness relation for galaxy clusters. (Rettura 2017)

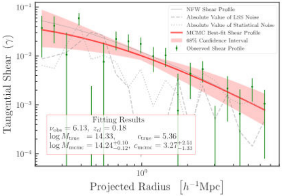

(b) Example of a shear profile around a galaxy cluster. (Chen et al. 2020)

Inferring cosmology from the Universe's mass distribution

Credit: Rubin Observatory/NSF/J. Pinto

(a) The principle of gravitational lensing.

Credit: NASA/ESA

(b) Weak and strong lensing in Abell 370.

What does lensing probe?

Lensing is a direct probe of the mass profiles and mass distribution of galaxies and galaxy clusters.

Weak lensing: a brief overview

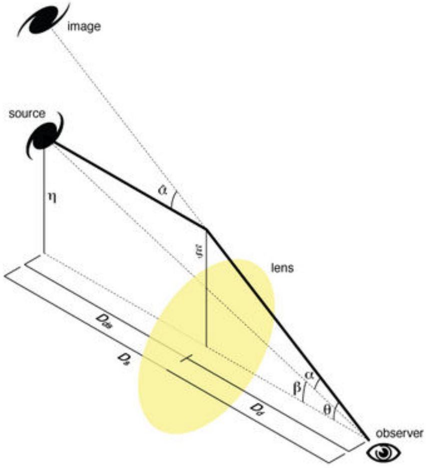

Figure 5: Definition of lensing angles and distances.
Figure by Michael SACHS

Lens equation

$$\vec{\beta} = \vec{\theta} - \frac{D_{ds}}{D_s}\hat{\alpha}(D_d\vec{\theta})$$

Magnification matrix

$$\frac{\partial \beta_i}{\partial \theta_j} = \delta_{ij} - \frac{\partial \alpha_i}{\partial \theta_j} = A_{ij}$$

Weak lensing hypotheses

- WL is perturbative
- Born approximation
- Thin & single lens approximations

Weak lensing: convergence, shear, and flexion

First order approximation of the magnification matrix

$$A = \begin{pmatrix} 1-\kappa & 0 \\ 0 & 1-\kappa \end{pmatrix} - \gamma \begin{pmatrix} \cos(2\phi) & \sin(2\phi) \\ \sin(2\phi) & -\cos(2\phi) \end{pmatrix}$$

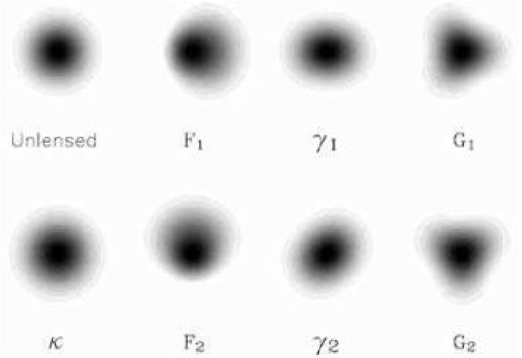

Figure 6: Effects of the different lensing fields on a Gaussian galaxy of radius 1 arcsec. 10% convergence/shear and 0.28 arcsec^{-1} flexion (which is a very high value for this quantity, chosen only to visualize) are applied. From Bacon et al. 2006

Weak lensing: going beyond the hypotheses

Weak lensing hypotheses

- WL is perturbative: all lensing effects are small
- Born approximation: small angles, evaluating deflections transversally
- Thin & single lens approximations: instant and successive deflections

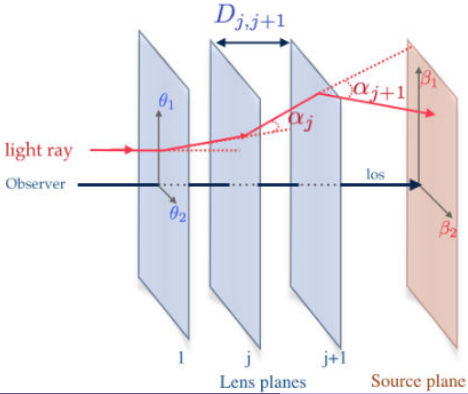

Figure 7: Raytracing in current cosmological simulations. Some hypotheses made are the thin lens and single lens approximations, along with the Born approximation. This framework of analysis can not generate strong lensing effects. Credit: C.Gouin

From "geometric" to relativistic lightcones

Current lightcone extraction

- Limited accuracy
- Simplified deflections
- Excluded strong lensing
- Non linearities?

Towards relativistic lightcones

- Full relativistic treatment
- Continuous deflections
- Weak and strong lensing
- GR handles non-linearities

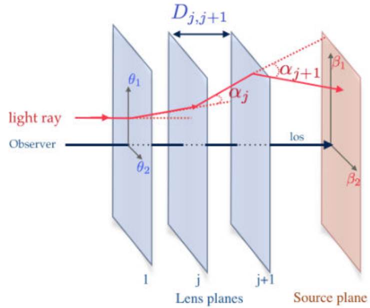

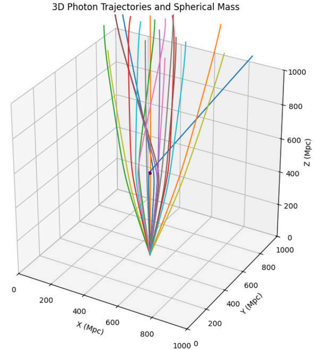

The homogeneous and isotropic Universe

The Friedmann-Lemaitre-Robertson-Walker metric

$$ds^2 = -c^2 dt^2 + a^2(t)\left[\frac{dr^2}{1-kr^2} + r^2(d\theta^2 + \sin^2\theta\, d\phi^2)\right]$$

where:

- $a(t)$: scale factor
- k: curvature parameter ($k = 0, +1, -1$)

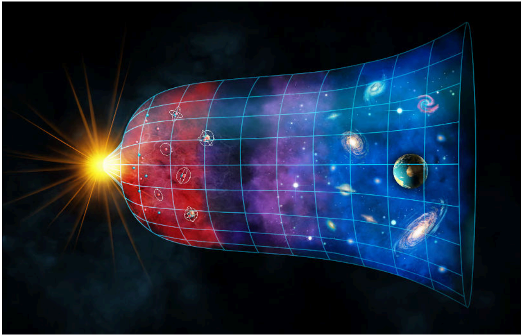

Figure 8: The story of the Universe: from the Big Bang to the present day.
Credit: Natalie Mayer

Perturbing the homogeneous and isotropic Universe

Perturbation of the FLRW metric

$$\mathrm{d}s^2 = -c^2(1 + 2\phi/c^2)\mathrm{d}t^2 - 2c \cdot a(t)B_i\mathrm{d}x^i\mathrm{d}t$$
$$- a^2(t)\left[(1 - 2\psi)\gamma_{ij} + 2E_{ij}\right]\mathrm{d}x^i\mathrm{d}x^j$$

where:

- ϕ: Newtonian potential
- B_i: vector potential
- ψ: spatial curvature perturbation
- E_{ij}: tensor perturbation
- γ_{ij}: spatial metric (flat, spherical, or hyperbolic)

From perturbations to trajectories

$$ds^2 = g_{\mu\nu}dx^\mu dx^\nu \Rightarrow \Gamma^\mu_{\alpha\beta} = \frac{1}{2}g^{\mu\nu}\left(\partial_\alpha g_{\nu\beta} + \partial_\beta g_{\nu\alpha} - \partial_\nu g_{\alpha\beta}\right)$$

The Christoffel symbols: geometry within dynamics

From this...

$$\Gamma^{\mu}_{\alpha\beta} = \frac{1}{2} g^{\mu\nu} \left(\partial_\alpha g_{\nu\beta} + \partial_\beta g_{\nu\alpha} - \partial_\nu g_{\alpha\beta} \right)$$

...

$$\Gamma^0_{ii} = \frac{1}{2} \Big[g^{00}(2\partial_i g_{i0} - \partial_0 g_{ii}) + g^{01}(2\partial_i g_{i1} - \partial_1 g_{ii}) + g^{02}(2\partial_i g_{i2} - \partial_2 g_{ii}) + g^{03}(2\partial_i g_{i3} - \partial_3 g_{ii}) \Big].$$

...

...to this!

$$\Gamma^0_{ii} = \frac{a\dot{a}}{c^2} + \frac{2a\dot{a}}{c^4}(\Phi + \Psi) - \frac{a^2}{c^4}\frac{\partial \Psi}{\partial t}$$

The Christoffel symbols: geometry within dynamics

Γ^0_{00}	$\frac{1}{c^2}\frac{\partial \Phi}{\partial t}$
Γ^i_{ii}	$-\frac{1}{c^2}\frac{\partial \Psi}{\partial x^i}$
Γ^0_{ii}	$\frac{a\dot{a}}{c^2} + \frac{2a\dot{a}}{c^4}(\Phi + \Psi) - \frac{a^2}{c^4}\frac{\partial \Psi}{\partial t}$
Γ^i_{00}	$\frac{1}{a^2}\frac{\partial \Phi}{\partial x^i}$
$\Gamma^0_{0i} = \Gamma^0_{i0}$	$\frac{1}{c^2}\frac{\partial \Phi}{\partial x^i}$
$\Gamma^i_{i0} = \Gamma^i_{0i}$	$\frac{\dot{a}}{a} - \frac{1}{c^2}\frac{\partial \Psi}{\partial t}$
Γ^i_{jj}	$\frac{1}{c^2}\frac{\partial \Psi}{\partial x^i}$
$\Gamma^i_{ij} = \Gamma^i_{ji}$	$-\frac{1}{c^2}\frac{\partial \Psi}{\partial x^j}$

Table 2: The perturbed Christoffel symbols in a flat spacetime, with vector and tensor perturbations set to zero. The terms $\dot{a}$ and a are the time derivative of the scale factor and the scale factor respectively.

The numerical tool EXCALIBUR

Geodesic equation in General Relativity: photon trajectory

$$\frac{d^2x^\mu}{d\lambda^2} + \Gamma^\mu_{\alpha\beta}\frac{dx^\alpha}{d\lambda}\frac{dx^\beta}{d\lambda} = 0$$

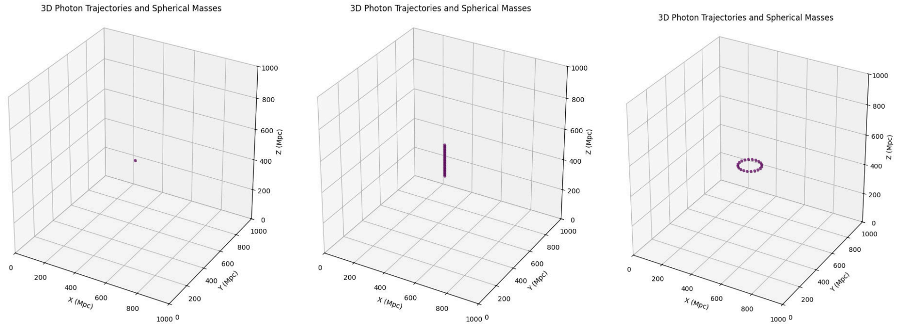

EXCALIBUR: **EX**act **CA**lculation of **LI**ght **B**ending **U**sing **R**elativity

A Python prototype for relativistic raytracing in a cosmological context.

What kind of geodesics?

Geodesic equation in General Relativity: photon trajectory

$$\frac{d^2x^\mu}{d\lambda^2} + \Gamma^\mu_{\alpha\beta}\frac{dx^\alpha}{d\lambda}\frac{dx^\beta}{d\lambda} = 0$$

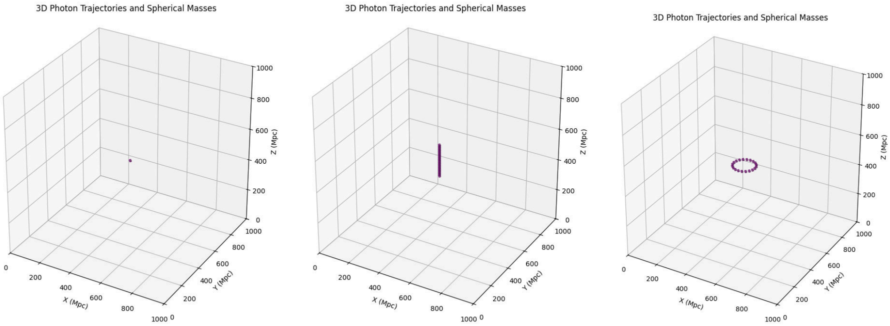

A fifth equation to rule them all

$$k^\mu k_\mu = 0$$

Geodesic equation in General Relativity: photon trajectory

$$\frac{d^2x^\mu}{d\lambda^2} + \Gamma^\mu_{\alpha\beta}\frac{dx^\alpha}{d\lambda}\frac{dx^\beta}{d\lambda} = 0$$

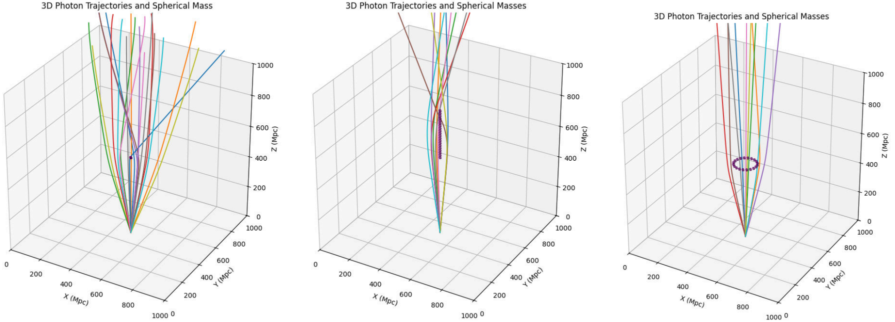

Figure 11: Simulations of geodesics deflected by masses in the Universe. Figures from the LAPP internship project. The sum of masses is always $10^{20} M_\odot$. From left to right: a single mass, a line of masses, and a ring-shaped mass distribution.

Relativistic light propagation and gravitational lensing

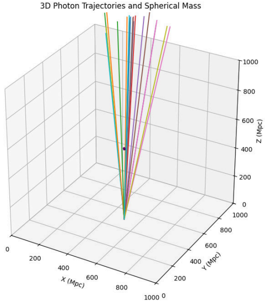

Figure 12: Simulation of geodesics deflected by a realistic mass ($10^{15} M_\odot$) in the Universe. Figure from the LAPP internship project.

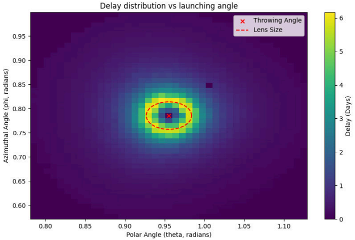

Figure 13: Time delay map for a realistic mass of $10^{15} M_\odot$ with a radius of 25 Mpc. The delay is measured between a deflected photon and a photon that would have traveled in a straight line. Figure from the LAPP internship project.

Relativistic light propagation and gravitational lensing

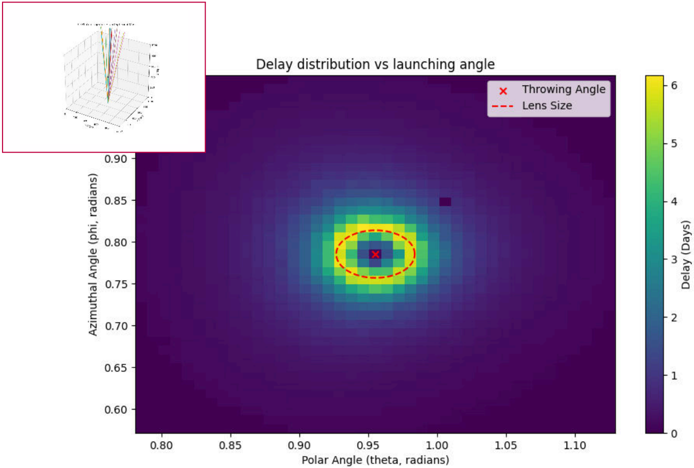

A weak but measurable effect

The time delay is of the order of a few days, which is very small compared to the time it takes for a photon to propagate (a few billion years).

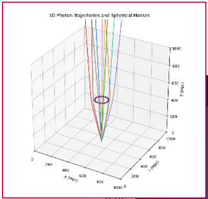

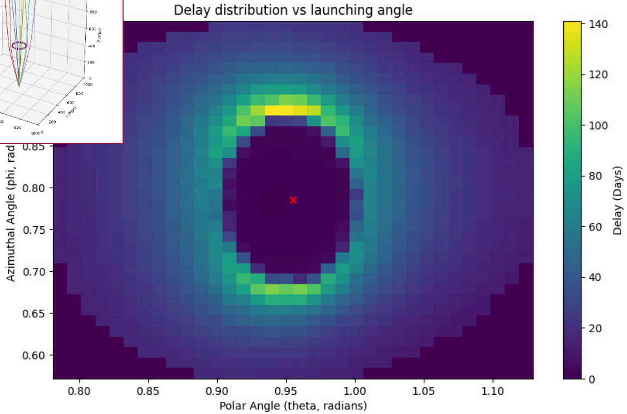

Different delay profiles for different mass distributions

The ring shape is clearly visible and rays that pass through the center are barely delayed, compared to the ones that pass closer to the ring.

Towards mass and radius estimations

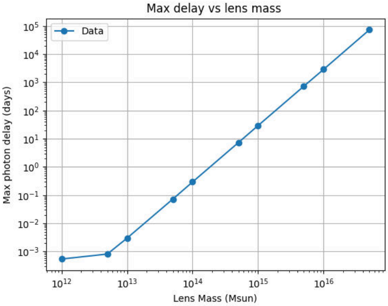

(a) Possibility to estimate the mass of the cluster based on the measured delay

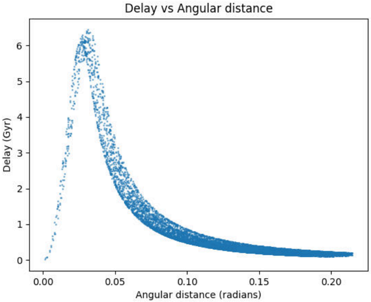

(b) Possibility to estimate the radius of the cluster based on the measured delay

Figure 14: First attempts at a calibration of mass and radius based on time delay measurements. Here, considered halos are spherical and assume constant density profiles. The plot on the right assumes a 25 Mpc radius and a mass of $10^{15} M_{\odot}$

Time delays in simulations: RayGal

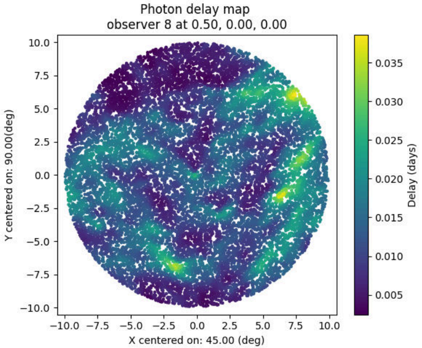

Figure 15: Delay maps obtained using the same process as before, this time on a snapshot from the cosmological simulation RayGal. For now, static Universe (photons integrated on only one snapshot), photons stopped on a sphere of radius 1 Gpc. Two different observers located at different points of the simulation box, both looking towards the center (0.5,0.5,0.5).

Perspectives: the numerical tool EXCALIBUR

Scaling **EXCALIBUR**

Translating from Python to C++ for performance. Scaling the code to run on modern cosmological simulations and make it ready to handle large datasets.

Going beyond the prototype

- Include the expansion of the Universe
- Include redshift studies
- Consider specific effects (moving sources,...)
- Extract lensing observables

Figure 16: CC-IN2P3, Lyon

Perspectives: a unified framework for relativistic effects

Credit: NASA

Galaxies' peculiar velocities

Credit: WMAP

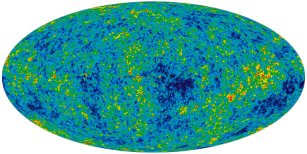

Integrated Sachs-Wolfe

$$G_{\mu\nu} = \frac{8\pi G}{c^4} T_{\mu\nu}$$

Credit: Andrea Danti

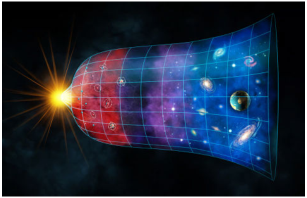

Universe expansion

Credit: ESA/HST

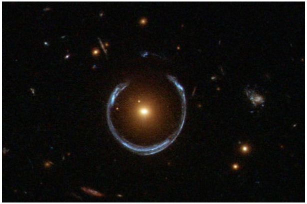

Gravitational lensing

A unified theoretical framework

Studying relativistic effects related to light propagation in cosmology.

Perspectives: making sense of the largest dataset yet

(a) The LSST telescope in Chile

Credit: Euclid/NASA/ESA/NRAO/AUI/NSF

Credit: Paulo Lago

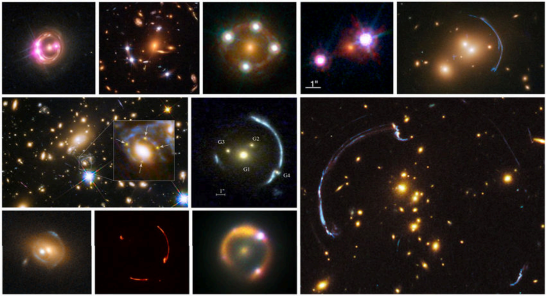

Perspectives: making sense of the largest dataset yet

Some key figures of the LSST project

- 3.2 billion pixels
- 8.4 m diameter mirror
- 10-year survey
- 20 TB of data per night
- 30 million objects detected per night
- Total survey area of 20,000 square degrees
- Tens of billions of galaxies ($\approx$ 10x more than previous surveys)
- Tens of thousands of strong lenses ($\approx$ 100x more)

Appendix: From Spherical to Cartesian coordinates

$$\bar{g}^{\text{sph}}_{\mu\nu} = \begin{bmatrix} -c^2 & 0 & 0 & 0 \\ 0 & \dfrac{a^2(t)}{1-kr^2} & 0 & 0 \\ 0 & 0 & a^2(t)r^2 & 0 \\ 0 & 0 & 0 & a^2(t)r^2\sin^2\theta \end{bmatrix}$$

$$r = \frac{\rho}{1+\frac{k}{4}\rho^2}$$

$$\bar{g}^{\text{cart}}_{\mu\nu} = \begin{bmatrix} -c^2 & 0 \quad 0 \quad 0 \\ 0 & \\ 0 & \dfrac{a^2(t)}{\left(1+\dfrac{k}{4}(x^2+y^2+z^2)\right)^2}\mathbb{I}_3 \\ 0 & \end{bmatrix}$$